Springer

KSME

Journal of Mechanical Science and Technology 30 (10) (2016) 4657~4667
www.springerlink.com/content/1738-494x(Print)/1976-3824(Online)
DOI 10.1007/s12206-016-0936-5

Elastic dynamic research of high-speed multi-link precision press considering structural stiffness of rotation joints †

Fengfeng Hu, Yu Sun* and Binbin Peng

School of Mechanical Engineering, Nanjing University of Science and Technology, Nanjing, 210094, China

(Manuscript Received November 13, 2015; Revised April 23, 2016; Accepted May 18, 2016)

Abstract

An elastic dynamic model of high-speed multi-link precision press considering structural stiffness of rotation joints was established by the finite element method. In the finite element model, rotation joint was established by four bar elements with equivalent stiffness, and connected link was established by beam element. Then, the elastic dynamics equation of the system was established, and modal superposition method was used to solve the dynamic response. Compared with the traditional elastic dynamic model with perfect constraint of the rotation joints, the elastic dynamic response value of the improved model is larger. To validate the presented new method of elastic dynamics analysis with stiffness of rotation joints, a related test of slider Bottom dead center (BDC) position in different speed was designed. The test shows that the model with stiffness of rotation joints is more reasonable. So it provides a reasonable theory and method for dynamic characteristics research of sucha multi-link machine.

Keywords: Dynamics; Multi-link press; Structural stiffness of rotation joints; Elastic dynamics; Dynamic response; Finite element

1. Introduction

With the development of aerospace, automobile, transportation and metallurgy, the high-speed precision press has been widely used. High speed, high precision and automation are the most important characteristics of the press. However, high-speed increases the inertial vibration force of motion links, which leads to the increase of elastic deformation and wave of links. Compared with the ideal curve, the motion curve of the slider has errors, which influences the dynamic characteristics and accuracy of the high speed press. To design a high speed and high precision multi-link press, the elastic deformation of motion links and motion pairs on their dynamic performance must be considered. The parameters of the joints, especially for kinematic joints, are very crucial for the machine tool dynamics, which is complicated and plays an important role in the surface quality and machining accuracy of the parts [1-3] and the stability of the machining process [4].

In the past several decades, several studies have focused on the definition of accurate mathematical models, both for single flexible body and multibody systems, by using the kineto-elasto (KED) dynamic analysis method, the Floating frame of reference (FFR) formulation, the incremental finite element method and the Absolute nodal coordinate formulation (ANCF). Mi et al. [5] analyzed the influence of preload of screw-nut joints and slider-guide joints on dynamic characteristics of a horizontal machining center. The results show that the preloads have significant effects on the horizontal machining center dynamic stiffness. To predict the dynamics of a high-speed machine tool, Zaghbani and Songmene [6] presented a methodology for estimating the machine tool modal parameters while the machine is operation by using operational modal analysis. As the different states will lead to different static and dynamic characteristics for machine tools, the finite element dynamic model based on single state cannot predict these variations. Lu et al. [7] built a model of a hybrid machine tool with three degrees of freedom and analyzed the static stiffness during the machining workspace based on the stiffness matrix. Van Brussel et al. [8] studied the dynamics of a three-axis machine tool by using Finite element method (FEM) and found that it possessed position-dependent dynamics. Symens [9] and Paijmans et al. [10] studied the dynamics variation in a machine with the position of the tool in its workspace for designing high-performance motion controllers. Erdman et al. [11, 12] proposed a kineto-elastodynamic approach based on flexibility matrix methods. Nath and Ghosh [13] presented a systematic finite element method for kineto-elastodynamic analysis of high speed mechanisms. In addition, the response of a slider-crank mechanism was found by Viscomi and Arye [14] to be dependent on five parameters classified as length, mass, damping, external piston force, and fre-

*Corresponding author. Tel.: +86 25 84315612, Fax.: +86 25 84315831
E-mail address: sunyu@mail.njust.edu.cn
† Recommended by Associate Editor Eung-Soo Shin

quency. Jou [15] and Fung [16, 17] refined the time-dependent boundary condition of the flexible connecting rod in a slider-crank mechanism and investigated the transient responses on the basis of different rotating speeds. Shabana and Yakoub [18, 19] studied the theoretical model of a three-dimensional beam element. They proposed a four-node beam element model by using several new nodal coordinates and verified the model with numerical simulations. Berzeri and Shabana [20, 21] analyzed the elastic forces of a beam element by decomposing the strain into the axial strain and the bending strain. The strain was described with various combinations of the simplified models of the axial strain and the bending strain. Sopanen and Mikkola [22] derived the mathematical formulation of the elastic forces of the three-dimensional beam element and examined the precision of the method with numerical simulations. Hussein et al. [23] studied the basic theory of some numerical methods for solving dynamic equations. The computational efficiency and accuracy of several implicit and explicit integration methods were compared. However, there is no detailed consideration of influence on the dynamic response for above documents by elastic properties of motion pairs. Most of them modeled motion pairs as perfect components, the constraints they impose on the behavior of the entire system are modeled through a set of perfect kinematic constraints.

Motion pairs are essential components of multibody systems, rigid or flexible. In fact, in most multibody systems, especially high speed precision machines, motion pairs modeled as perfect ones are not appropriate. In actual joints, clearance, friction, lubrication and stiffness will play an important role and can have a significant effect on the dynamic response of the system [24]. For instance, caused by the structural characteristics and material characteristics of bearing bush, maybe stiffness of the motion pair is lower than flexibility link, so modeled joints as perfect components cannot really reflect the mechanism dynamic characteristics. Ravn [25] and co-workers studied the effect of clearance on system response, including the effect of lubrication and link flexibility, but they ignored the elastic deformation of motion pairs. Dubowsky, Deck and co-workers [26, 27] considered the effect of link flexibility for both planar and spatial cases with joints characteristics; they only used an approximate formula to express the contact stiffness between the journal and bearing bush but ignored structural characteristics.

In the present formulation, elastic bodies are modeled by using the finite element method. For beam elements, the location of each node is represented by its Cartesian coordinates in an inertial frame, and the rotation of the cross-section at each node is represented by a finite rotation tensor expressed in the same inertial frame. The kinematic constraints among the various bodies are enforced via the Lagrange multiplier technique. Although this approach does not involve a minimum set of coordinates, it allows a modular development of finite elements for the enforcement of the kinematic constraints [28, 29].

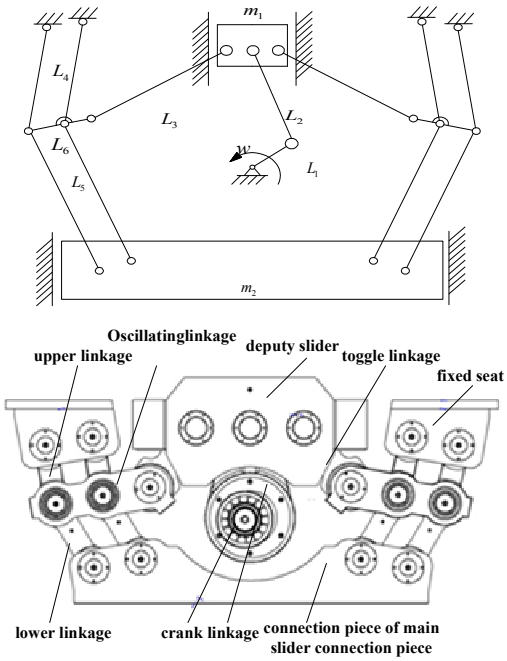

Fig. 1. A new type of high speed multi-link press.

In the view of the lack previous research on rotation joints stiffness, the equivalent structural stiffness of rotation joint was accurately calculated by using the finite element statics calculation first. Then a complex elastic dynamic model of a high-speed multi-link press with the rotation joints characters was established by finite element method, where rotation joint is equivalent to bar element with appropriate stiffness. And elastic dynamic response of the complex elastic dynamic equation was solved by modal superposition method. Lastly, the results of the new model were compared with the traditional kineto-elasto dynamic analysis method with perfect constraint of joints. To prove the accuracy of the new model, a related test was designed and tested.

2. Elastic dynamics modeling of multi-link press

2.1 Multi-link press model

The principle of a new type of high speed multi-link press is shown as in Fig. 1. The press with a set of slider-crank mechanism is the first level of transmission of the crankshaft (L1, L2 and m1). Toggle links (L3) are symmetrically distributed on both sides of the movement axis of the slider. One end of the toggle is connected to deputy slider (m1), and the other is connected to oscillating link (L6). Upper end of upper link (L4) is connected to the fuselage, and its lower end is connected to the oscillating link. Upper end of lower link (L5) is connected to oscillating link, and its lower end is connected to main slider (m2). Thus, a completely closed loop transmission structure is created. Deputy slider does reciprocating motion in vertical direction driven by the crankshaft (L1). Links on both sides of the mechanism do synchronous oscillation in plane by further driving of toggle links. Finally, they realize

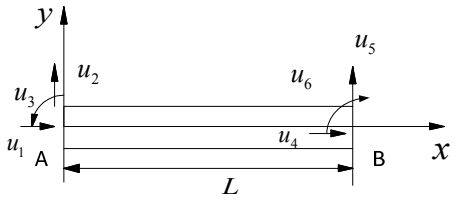

Fig. 2. Beam element and its coordinate relations.

the main slider movement.

2.2 Finite element model of connected link

As shown in Fig. 2, a uniform-section beam element is used to simulate flexible links of the mechanism. The horizontal and vertical displacements of beam unit are both unit coordinate function $\bar{x}$ and a function of time t. The horizontal and vertical displacements of an arbitrary point are named as W (t) and V (t), respectively. The longitudinal and lateral displacements are all described by using third-order liner polynomials.

$$\begin{cases} W(x,t) = a_0 + a_1 x + a_2 x^2 + a_3 x^3 \\ V(\bar{x},t) = b_0 + b_1 x \end{cases} . \tag{1}$$

There are a total of six undetermined parameters in the formulas above, so eight generalized coordinates in the node A and B of the beam element need to be set.

The generalized coordinates array of the element with six generalized coordinates form is as follows:

$$\boldsymbol{u} = \left[u_1 \quad u_2 \quad \cdots \quad u_6 \right]^T .$$

Each of undetermined coefficients of Eq. (1) can be obtained according to the boundary conditions as follows:

$$\begin{aligned} &V(0,t) = u_1(t) \quad V(L,t) = u_4(t) \\ &W(0,t) = u_2(t) \quad W(L,t) = u_5(t) \\ &\dot{W}(0,t) = u_3(t) \quad \dot{W}(L,t) = u_6(t) . \end{aligned}$$

2.3 Finite element model of rotation joints

Generally, the linkages between each joint, connecting rod and the rack are connected with bearings. But it is difficult to establish accurate motion components (bearings, journals, rack, etc.) and consider various nonlinear factors such as contact, stiffness and clearance in an elastic dynamic system of multi-link press. There is no doubt that it increases the difficulty of the system modeling and solving. In addition, in our machine, the surface coarse degree of the bearing bush is low and the friction coefficient is small, so the contact friction is relatively small between journal and bearing bush. Particularly, compared with elastic deformation caused by inertia force, the dynamic response of slider vertical direction influenced by frictional force is smaller. Therefore, this paper makes the following equivalent hypothesis: the friction between journal and bearing is ignored, rotation joints only have radial force. The rigidity characteristics of rotation joint are obtained by finite element statics analysis. Then a rotation joint is equivalent to the corresponding four bar elements. So it can be formed to the overall elastic system dynamic model.

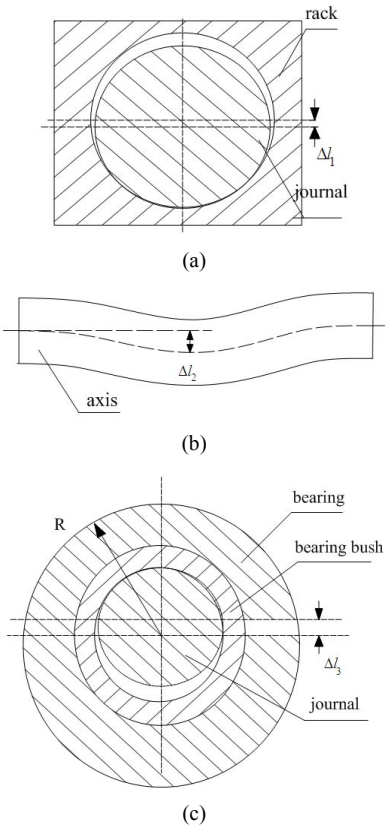

Fig. 3. (a) The elastic deformation of frame; (b) bending deformation of the journal; (c) tensile or compressive elastic deformation of bearing and bearing bush.

2.3.1 Equivalent model of rotation joints

Rotation joint consists of journal, bearing and bearing bush. Under the action of axial force, journal comes into being bending deformation, and bearing, bearing bush are stretched or compressed into an oval as shown in the figures below.

So the total deformation of the rotation joint can be approximated to:

$$\Delta L = \Delta l_1 + \Delta l_2 + \Delta l_3 . \tag{2}$$

The equivalent strain of rotation joint is:

$$\bar{\varepsilon} = \frac{\Delta L}{R} . \tag{3}$$

So stiffness characteristics of rotation joint are replaced by bar element. As shown in the figure below is a bar element with two nodes A, B in its both ends. Assuming that longitu-

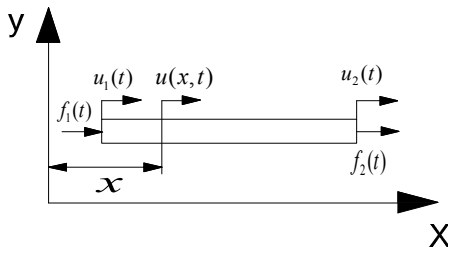

Fig. 4. Equivalent bar element.

dinal displacement in node A and B are $u_1(t)$ and $u_2(t)$. Two nodes are effect by axial force $f_1(t)$ and $f_2(t)$, respectively. $u(x,t)$ express any location of the longitudinal displacement.

Unit elastic dynamics equation is obtained in the same way based on Lagrange analysis method as follows:

$$\bar{m}\ddot{u} + \bar{k}u = \bar{f}\,. \tag{4}$$

To establish the system differential equations, the matrix is extended as follows:

$$\bar{\boldsymbol{m}} = \bar{\rho}AL\begin{bmatrix} \frac{1}{3} & 0 & 0 & \frac{1}{6} & 0 & 0 \\ & 0 & 0 & 0 & 0 & 0 \\ & & 0 & 0 & 0 & 0 \\ & & & \frac{1}{3} & 0 & 0 \\ & & & & 0 & 0 \\ (sym.) & & & & & 0 \end{bmatrix},$$

$$\bar{\boldsymbol{k}} = \bar{E}\begin{bmatrix} \frac{A}{L} & 0 & 0 & -\frac{A}{L} & 0 & 0 \\ & 0 & 0 & 0 & 0 & 0 \\ & & 0 & 0 & 0 & 0 \\ & & & \frac{A}{L} & 0 & 0 \\ & & & & 0 & 0 \\ (sym.) & & & & & 0 \end{bmatrix},$$

$$u = \begin{bmatrix} u_1(t) & 0 & 0 & 0 & u_2(t) & 0 & 0 & 0 \end{bmatrix},$$

$$\bar{f} = \begin{bmatrix} f_1(t) & 0 & 0 & 0 & f_2(t) & 0 & 0 & 0 \end{bmatrix}.$$

Equivalent bar element is regarded as the lightweight pole, which is similar to the spring. And the quality of joint is put on the corresponding node in the form of concentrated mass

$$\bar{E}\varepsilon = \frac{F}{A}\,. \tag{5}$$

Substituting Eq. (3) into Eq. (5):

$$\bar{E} = \frac{F \times R}{A \times \Delta L}. \tag{6}$$

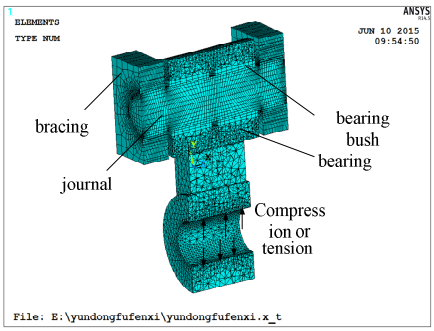

Fig. 5. Mesh generation.

So the equivalent bar element model and its corresponding parameters are obtained.

The element generalized coordinates under absolute coordinates are as follows:

$$\boldsymbol{U}_b^e = \begin{bmatrix} U_{b1} & 0 & 0 & U_{b4} & 0 & 0 \end{bmatrix}^T.$$

So the unit movement differential equation of rotation joint equivalent element under absolute reference frame is obtained.

$$\boldsymbol{m}_b\ddot{\boldsymbol{U}}_b^e + \boldsymbol{k}_b\boldsymbol{U}_b^e = \boldsymbol{f}_b \tag{7}$$

where

$$\boldsymbol{m}_b = \boldsymbol{R}^T\bar{\boldsymbol{m}}\boldsymbol{R} \tag{8}$$

$$\boldsymbol{k}_b = \boldsymbol{R}^T\bar{\boldsymbol{k}}\boldsymbol{R} \tag{9}$$

$$\boldsymbol{f}_b = \boldsymbol{R}^T\bar{\boldsymbol{f}}\,. \tag{10}$$

2.3.2 Stiffness calculation of rotation joints

Statics analysis of the rotation joint is done by ANSYS. Solid185 is chosen as the unit type. The elasticity modulus E of journal, bearing and link (Material for them is 40Cr) is 2.1ell Pa. And the elasticity modulus E of bearing bush (Material for it is ZCuPb10Sn10) is 1.15ell Pa. Poisson's ratio ς is 0.28. Mesh generation is shown in the following figure.

Deformation results of rotation joint are calculated as shown in Fig. 6 when the applied force on the journal is 15 tons.

According to the deformation nephogram and Sec. 2.3.1, the general equivalent deformation of rotation joint with 15 tons of tension is as follows:

$$\Delta L_{\ t} = \Delta l_1 + \Delta l_2 + \Delta l_3 = 6.94 \times 10^{-5} m.$$

Equivalent strain:

$$\bar{\varepsilon}_{\ t} = \frac{\Delta L_t}{R} = \frac{6.94 \times 10^{-5} m}{1.4 \times 10^{-1} m} = 4.96e-04.$$

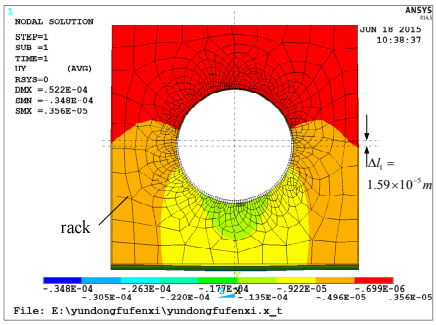

(a)

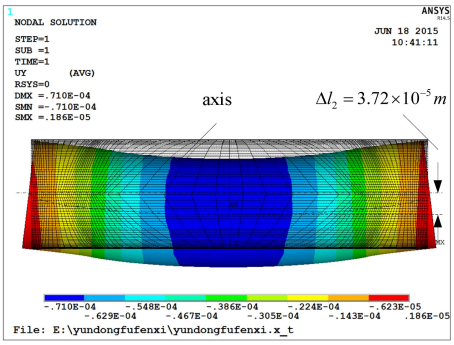

(b)

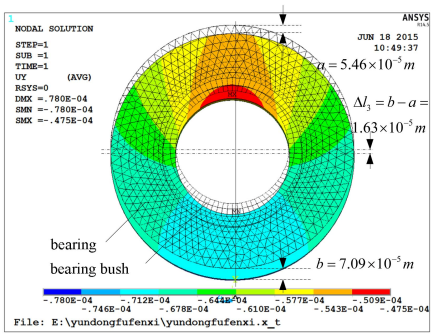

(c)

Fig. 6. (a) Elastic deformation of shaft support; (b) elastic deformation of journal; (c) elastic deformation of bearing and bearing bush.

Equivalent elastic modulus:

$$\overline{E}_t = \frac{F}{A\times\overline{\varepsilon}_t} = \frac{1.5\times10^5 N}{9\times10^{-4} m^2 \times 4.96\times10^{-4}} = 3.36\times10^{11} N/m^2 .$$

Similarly, equivalent deformation and the equivalent elastic modulus with 15 tons of pressure are as follows:

$$\Delta L_c = 4.32\times10^{-5} m$$
$$\overline{E}_c = 5.40\times10^{11} N/m^2 .$$

So, values of the equivalent modulus of elasticity in the model can be obtained:

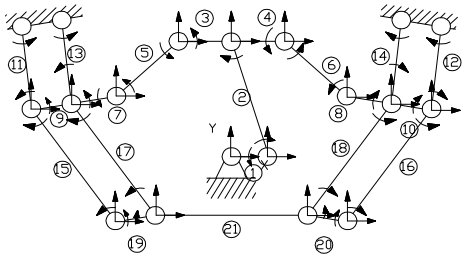

Fig. 7. Elastic dynamics model of the mechanism with perfect kinematic constraints.

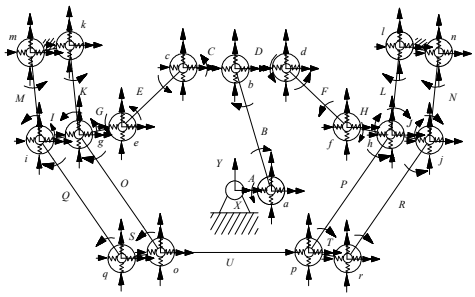

Fig. 8. Elastic dynamics model of the mechanism with rotation joints deformation.

$$\overline{E}_{\text{I or III}} = \begin{cases} \overline{E}_t/2 = 1.68\times10^{11}, & if \quad F_N \ge 0 \\ \overline{E}_c/2 = 2.7\times10^{11}, & if \quad F_N < 0 \end{cases}$$
$$\overline{E}_{\text{II or IV}} = \frac{\overline{E}_t + \overline{E}_c}{4} = 2.17\times10^{11} .$$

The bar linkage is tensile when $F_N \ge 0$. However, the bar linkage is compressive when $F_N < 0$. Stiffness of rotation joint perpendicular to the axial is assumed as the average of $\overline{E}_t$ and $\overline{E}_c$.

2.4 Differential equation of system movement

According to the traditional theory of elastic dynamics model with perfect kinematic constraints, the elastic dynamics model of the mechanism in Fig. 1 is established with 21 elements, 19 nodes, 67 degrees of freedom elastic dynamic model as shown in Fig. 7.

According to the theory of elastic dynamics research with the stiffness of rotation joint, the elastic dynamics model of the mechanism in Fig. 1 is established with 93 elements, 91 nodes, 104 degrees of freedom elastic dynamic model as shown in Fig. 8.

Relationship between the generalized coordinates of dynamical model with link and rotation joint, such as the links C, E and the rotation joint c between them, is shown as follows:

Relationship of generalized coordinates between the rotation joint and links is as follows:

$$U_{\text{c III}} = U_{\text{c IV2}} = U_{C4}$$
$$U_{\text{c II}} = U_{\text{c III2}} = U_{C5}$$

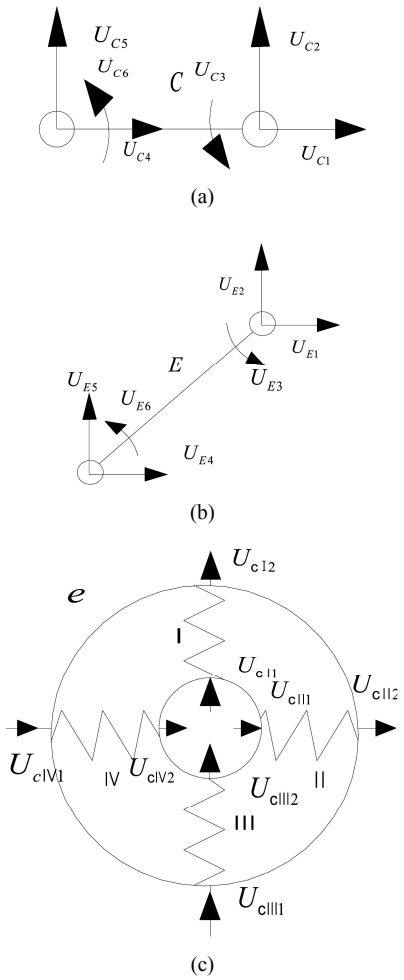

Fig. 9. (a) System generalized coordinates of link C; (b) system generalized coordinates of link E; (c) system generalized coordinates of rotation joint e.

$$U_{cII2} = U_{cIV1} = U_{E1}$$
$$U_{cI2} = U_{cIII1} = U_{E2}.$$

The movement differential equation of the system can be obtained after all equations of these elements are given. The motion differential equation of the element i is as follows.

$$\boldsymbol{m}_{ai}\ddot{\boldsymbol{U}}_{ai}^{e} + \boldsymbol{k}_{ai}\boldsymbol{U}_{ai}^{e} = \boldsymbol{f}_{ai} - \boldsymbol{m}_{ai}\ddot{\boldsymbol{U}}_{ari}^{e} \tag{11}$$

or

$$\boldsymbol{m}_{bi}\ddot{\boldsymbol{U}}_{bi}^{e} + \boldsymbol{k}_{bi}\boldsymbol{U}_{bi}^{e} = \boldsymbol{f}_{bi}. \tag{12}$$

Define array for rigid body acceleration of the system can be shown as:

$$\ddot{\boldsymbol{U}}_{ar} = \left[\ddot{U}_{ar1} \quad \ddot{U}_{ar2} \quad \cdots \quad \ddot{U}_{arNu}\right]^{T}.$$

The array $\ddot{\boldsymbol{U}}_{ar}$ and $\boldsymbol{U}$ has the same dimension. $\boldsymbol{U}_{(a\,or\,b)i}^{e}$ is a six-dimension array, and $\boldsymbol{U}$ is an $\boldsymbol{N}_u$ dimension array, and the former is only part of the latter. The relationship between them is listed as follows:

$$\boldsymbol{U}_{(a\,or\,b)i}^{e} = \boldsymbol{B}_i\boldsymbol{U} \tag{13}$$
$$\boldsymbol{B}_i\left(k, \boldsymbol{I}_u(i,k)\right) = 1. \tag{14}$$

So

$$\boldsymbol{M}_{ai}^{e}\boldsymbol{U} + \boldsymbol{K}_{ai}^{e}\boldsymbol{U} = \boldsymbol{F}_{ai}^{e} - \boldsymbol{M}_{ai}^{e}\ddot{\boldsymbol{U}}_{ar} \tag{15}$$

or

$$\boldsymbol{M}_{bi}^{e}\boldsymbol{U} + \boldsymbol{K}_{bi}^{e}\boldsymbol{U} = \boldsymbol{F}_{bi}^{e} \tag{16}$$

where

$$\boldsymbol{M}_{(a\,or\,b)i}^{e} = \boldsymbol{B}_i^{T}\boldsymbol{m}_{(a\,or\,b)i}\boldsymbol{B}_i \tag{17}$$
$$\boldsymbol{K}_{(a\,or\,b)i}^{e} = \boldsymbol{B}_i^{T}\boldsymbol{k}_{(a\,or\,b)i}\boldsymbol{B}_i \tag{18}$$
$$\boldsymbol{F}_{(a\,or\,b)i}^{e} = \boldsymbol{B}_i^{T}\boldsymbol{f}_{(a\,or\,b)i}. \tag{19}$$

After adding up all motion equations of elements under the generalized coordinates, the motion differential equation of the system is established.

$$\boldsymbol{M}\ddot{\boldsymbol{U}} + \boldsymbol{K}\boldsymbol{U} = \boldsymbol{F} - \boldsymbol{M}\ddot{\boldsymbol{U}}_{r} \tag{20}$$

where

$$\begin{cases} \boldsymbol{M} = \sum_{i=1}^{Ne}\boldsymbol{M}_{ai}^{e} + \sum_{i=1}^{Ne}\boldsymbol{M}_{bi}^{e} \\ \boldsymbol{K} = \sum_{i=1}^{Ne}\boldsymbol{K}_{ai}^{e} + \sum_{i=1}^{Ne}\boldsymbol{K}_{bi}^{e} \\ \boldsymbol{F} = \sum_{i=1}^{Ne}\boldsymbol{F}_{ai}^{e} + \sum_{i=1}^{Ne}\boldsymbol{F}_{bi}^{e}. \end{cases} \tag{21}$$

The kinetic energy of the elements distributed quality is only considered in analysis of the system mass matrix, and some kinetic energy of concentrated parameters is not considered, such as quality of rotation joints, quality of the slider and so on. For these concentrated parameters which should be superimposed to the mass matrix, the system mass matrix is revised as follows:

$$\boldsymbol{M} = \boldsymbol{M}_c + \sum_{i=1}^{Ne}\boldsymbol{M}_{ai}^{e} + \sum_{i=1}^{Ne}\boldsymbol{M}_{bi}^{e}. \tag{22}$$

Considering the damping effect in Eq. (20), the movement differential equation of the system is established as follows:

$$\boldsymbol{M}\ddot{\boldsymbol{U}} + \boldsymbol{C}\dot{\boldsymbol{U}} + \boldsymbol{K}\boldsymbol{U} = \boldsymbol{F} - \boldsymbol{M}\ddot{\boldsymbol{U}}_{r}. \tag{23}$$

3. Numerical solutions of elastic dynamics

3.1 Multi degree of freedom vibration equation decoupling based on the modal superposition method

As mentioned above, Nth natural frequency and the corresponding dominant vibration modes $\boldsymbol{A}_r$ (r = 1, 2,..., n) can be obtained through Eqs. (24) and (25). Regularization processing of principal mode vector is done first. Assuming that:

$$\boldsymbol{\varphi}_r = \frac{1}{C_r}\boldsymbol{A}_r \tag{24}$$

where $C_r = \sqrt{\boldsymbol{A}_r^T \boldsymbol{M}\boldsymbol{A}_r}$ is referred to the regularization factor. $\boldsymbol{\varphi}_r$ is rth regularization mode which satisfies the following conditions:

$$\boldsymbol{\varphi}_r^T \boldsymbol{M}\boldsymbol{\varphi}_r = 1. \tag{25}$$

Regular modal matrix $\boldsymbol{\Phi}$ is made up after the regularization processing of nth order principal mode.

$$\boldsymbol{\Phi} = \begin{bmatrix}\boldsymbol{\varphi}_1 & \boldsymbol{\varphi}_2 & \cdots & \boldsymbol{\varphi}_n\end{bmatrix}. \tag{26}$$

By using regular modal matrix, the system mass matrix can be translated into a unit matrix, and system stiffness matrix can be translated into a diagonal matrix.

$$\boldsymbol{\Phi}^T \boldsymbol{M}\boldsymbol{\Phi} = \boldsymbol{I} \tag{27}$$

$$\boldsymbol{\Phi}^T \boldsymbol{K}\boldsymbol{\Phi} = \boldsymbol{\Omega} = \begin{bmatrix}\omega_1^2 & & & \\ & \omega_2^2 & & \\ & & \ddots & \\ & & & \omega_n^2\end{bmatrix}. \tag{28}$$

Because each regular modal vector is linearly independent and can be used as a set of basal of n dimensional linear space, so any vector of the space can be regarded as the linear combination of the basal. The system of generalized coordinates vector U is expressed as below:

$$\boldsymbol{U} = \eta_1\boldsymbol{\varphi}_1 + \eta_2\boldsymbol{\varphi}_2 + \cdots + \eta_n\boldsymbol{\varphi}_n = \boldsymbol{\Phi}\boldsymbol{\eta} \tag{29}$$

where

$$\boldsymbol{\eta} = \begin{bmatrix}\eta_1 & \eta_2 & \cdots & \eta_n\end{bmatrix}^T.$$

Therefore, the system of non-damping free vibration equations can be transformed into the following equation:

$$\boldsymbol{\Phi}^T \boldsymbol{M}\boldsymbol{\Phi}\ddot{\boldsymbol{\eta}} + \boldsymbol{\Phi}^T \boldsymbol{K}\boldsymbol{\Phi}\boldsymbol{\eta} = 0. \tag{30}$$

Considering Eqs. (26) and (27)

$$\ddot{\boldsymbol{\eta}} + \boldsymbol{\Omega}\boldsymbol{\eta} = 0. \tag{31}$$

Eq. (31) can be expanded for many independent equations because Ω is a diagonal matrix.

$$\begin{cases}\ddot{\eta}_1 + \omega_1^2\eta_1 = 0 \\ \ddot{\eta}_2 + \omega_2^2\eta_2 = 0 \\ \quad\vdots \\ \ddot{\eta}_n + \omega_n^2\eta_n = 0.\end{cases} \tag{32}$$

So, decoupling of the multi degree of freedom vibration equation is realized. The problem of n degrees of freedom vibration is converted to the superposition of n independent single degree of freedom vibration equations.

3.2 Assumption of regular modal damping

The decoupling theory above is mainly for no-damping free vibration model of the system. But in the process of practical work, the elastic component is always affected by various damping effects. Therefore, the damping must be considered when the dynamic response of the structure is calculated.

Because the reasons for damping are various, in most cases, the damping principle cannot be known exactly, and the form of system damping matrix $\boldsymbol{C}$ is difficult to determine. Considered from the perspective of easy to solve, the damping matrix is assumed to be a linear combination of system mass matrix and stiffness matrix in the process of analysis

$$\boldsymbol{C} = \alpha\boldsymbol{M} + \beta\boldsymbol{K} \tag{33}$$

where α and β are constant.

Assuming that

$$\bar{\boldsymbol{C}} = \alpha\boldsymbol{I} + \beta\boldsymbol{\Omega}. \tag{34}$$

So

$$\bar{\boldsymbol{C}} = \boldsymbol{\Phi}^T \boldsymbol{C}\boldsymbol{\Phi} = \begin{bmatrix}2\zeta_1\omega_1 & & & \\ & 2\zeta_2\omega_2 & & \\ & & \ddots & \\ & & & 2\zeta_n\omega_n\end{bmatrix}. \tag{35}$$

This damping matrix is called a regular damping matrix. where, $\xi_1\xi_2...\xi_n$ is the damping ratio. Therefore, the free vibration equation of the system considering the damping effect is translated into as below:

$$\ddot{\boldsymbol{\eta}} + \bar{\boldsymbol{C}}\dot{\boldsymbol{\eta}} + \boldsymbol{\Omega}\boldsymbol{\eta} = 0. \tag{36}$$

It is easy to see that the introduction of regular damping matrix in the form of diagonal matrix can make the equation above uncoupled. That can be written as n single degree of freedom damped vibration equations. And the damping ratio is assumed as 0.05 [30].

$$\begin{cases} \ddot{\eta}_1 + 2\zeta_1\omega_1\dot{\eta}_1 + \omega_1^2\eta_1 = 0 \\ \ddot{\eta}_2 + 2\zeta_2\omega_2\dot{\eta}_2 + \omega_2^2\eta_2 = 0 \\ \vdots \\ \ddot{\eta}_n + 2\zeta_n\omega_n\dot{\eta}_n + \omega_n^2\eta_n = 0. \end{cases} \tag{37}$$

3.3 Real kinematic solution of the mechanism

This section introduces a method to solve the dynamic response of each cycle. The basic idea is similar to modal superposition method in solving the multi degree of freedom system vibration equation. The process solves the characteristic value for system natural frequency and vibration mode, decoupling the equation, and working out vibration coordinates of several minimum modes of vibration. Then the generalized coordinates are reversely solved. As the mechanism is a time-varying system; the exercise period T of the system is divided into n time unit. In each time unit, the mechanism is used as fixed-length system. Step length of each time unit is as follows:

$$\Delta t = T / n. \tag{38}$$

Considering the ith time unit $(t_{i-1} \le t \le t_i)$, the mass matrix and stiffness matrix of the system take the value in start time of the unit, and keep to $M^{(i)}$, $K^{(i)}$. Each natural frequency and the corresponding vector of each vibration mode at the moment are obtained by solving the characteristic value. So the decoupled equation of each mode is as follows:

$$\ddot{\eta}_r(t) + 2\zeta_r\omega_r^{(i)}\dot{\eta}_r(t) + \left(\omega_r^{(i)}\right)^2\eta_r(t) = N_r(t) \tag{39}$$

If the response $\eta_r(t_{i-1})$, $\dot{\eta}_r(t_{i-1})$ of the ith time unit at starting time t_{i-1} is known, it can be solved as below:

$$\eta_r(t_i) = \frac{1}{\omega_{dr}^{(i)}}\int_{t_{i-1}}^{t_i} N_r(\tau)\mathrm{e}^{-\zeta_r\omega_r^{(i)}(t_i-\tau)}\sin\omega_{dr}^{(i)}(t_i-\tau)\mathrm{d}\tau + \frac{\eta_r(t_{i-1})}{\sqrt{1-\zeta_r^2}}\mathrm{e}^{-\zeta_r\omega_r^{(i)}\Delta t}\cos(\omega_{dr}^{(i)}\Delta t - \psi_r) + \frac{\eta_r(t_{i-1})}{\omega_{dr}^{(i)}}\mathrm{e}^{-\zeta_r\omega_r^{(i)}\Delta t}\sin\omega_{dr}^{(i)}\Delta t \tag{40}$$

$$\dot{\eta}_r(t_i) = \frac{1}{\omega_{dr}^{(i)}}\int_{t_{i-1}}^{t_i} N_r(\tau)\left[-\zeta_r\omega_r^{(i)}\mathrm{e}^{-\zeta_r\omega_r^{(i)}(t_i-\tau)}\sin\omega_{dr}^{(i)}(t_i-\tau) + \omega_{dr}^{(i)}\mathrm{e}^{-\zeta_r\omega_r^{(i)}(t_i-\tau)}\cos\omega_{dr}^{(i)}(t_i-\tau)\right]\mathrm{d}\tau - \eta_r(t_{i-1})\left[\frac{\omega_{dr}^{(i)}}{\sqrt{1-\zeta_r^2}}\mathrm{e}^{-\zeta_r\omega_r^{(i)}\Delta t}\sin(\omega_{dr}^{(i)}\Delta t - \psi_r) + \frac{\zeta_r\omega_r^{(i)}}{\sqrt{1-\zeta_r^2}}\mathrm{e}^{-\zeta_r\omega_r^{(i)}\Delta t}\cos(\omega_{dr}^{(i)}\Delta t - \psi_r)\right] - \dot{\eta}_r(t_{i-1})\left[\frac{\zeta_r\omega_r^{(i)}}{\omega_{dr}^{(i)}}\mathrm{e}^{-\zeta_r\omega_r^{(i)}\Delta t}\sin\omega_{dr}^{(i)}\Delta t - \mathrm{e}^{-\zeta_r\omega_r^{(i)}\Delta t}\cos\omega_{dr}^{(i)}\Delta t\right]. \tag{41}$$

Eqs. (40) and (41) can be converted into the form of linear equation as follows:

$$\begin{cases} a_1^{(i)}\eta(t_{i-1}) + b_1^{(i)}\dot{\eta}(t_{i-1}) + c_1^{(i)}\eta(t_i) + d_1^{(i)}\dot{\eta}(t_i) = e_1^{(i)} \\ a_2^{(i)}\eta(t_{i-1}) + b_2^{(i)}\dot{\eta}(t_{i-1}) + c_2^{(i)}\eta(t_i) + d_2^{(i)}\dot{\eta}(t_i) = e_2^{(i)} \end{cases} \tag{42}$$

where

$$a_1^{(i)} = -\frac{1}{\sqrt{1-\zeta_r^2}}\mathrm{e}^{-\zeta_r\omega_r^{(i)}\Delta t}\cos(\omega_{dr}^{(i)}\Delta t - \psi_r)$$

$$b_1^{(i)} = -\frac{1}{\omega_{dr}^{(i)}}\mathrm{e}^{-\zeta_r\omega_r^{(i)}\Delta t}\sin\omega_{dr}^{(i)}\Delta t$$

$$c_1^{(i)} = 1$$

$$d_1^{(i)} = 0$$

$$e_1^{(i)} = \frac{1}{\omega_{dr}^{(i)}}\int_{t_{i-1}}^{t_i} N_r(\tau)\mathrm{e}^{-\zeta_r\omega_r^{(i)}(t_i-\tau)}\sin\omega_{dr}^{(i)}(t_i-\tau)\mathrm{d}\tau$$

$$a_2^{(i)} = \omega_r^{(i)}\mathrm{e}^{-\zeta_r\omega_r^{(i)}\Delta t}\left[\sin(\omega_{dr}^{(i)}\Delta t - \psi_r) + \frac{\zeta_r}{\sqrt{1-\zeta_r^2}}\cos(\omega_{dr}^{(i)}\Delta t - \psi_r)\right]$$

$$b_2^{(i)} = \mathrm{e}^{-\zeta_r\omega_r^{(i)}\Delta t}\left[\frac{\zeta_r}{\sqrt{1-\zeta_r^2}}\sin\omega_{dr}^{(i)}\Delta t - \cos\omega_{dr}^{(i)}\Delta t\right]$$

$$c_2^{(i)} = 0$$

$$d_2^{(i)} = 1$$

$$e_2^{(i)} = \int_{t_{i-1}}^{t_i} N_r(\tau)\left[-\frac{\zeta_r}{\sqrt{1-\zeta_r^2}}\mathrm{e}^{-\zeta_r\omega_r^{(i)}(t_i-\tau)}\sin\omega_{dr}^{(i)}(t_i-\tau) + \mathrm{e}^{-\zeta_r\omega_r^{(i)}(t_i-\tau)}\cos\omega_{dr}^{(i)}(t_i-\tau)\right]\mathrm{d}\tau.$$

In addition, considering the periodic system motion state, there are the following boundary conditions:

$$\begin{cases} \eta_r(t_n) = \eta_r(t_0) \\ \dot{\eta}_r(t_n) = \dot{\eta}_r(t_0). \end{cases} \tag{43}$$

Further changes of the generalized coordinates of U can be calculated by Eq. (29).

$$\boldsymbol{U}(t) = \sum_{r=1}^{n_r}\eta_r(t)\boldsymbol{\varphi}_r. \tag{44}$$

3.4 Elastic dynamic response of the slider vertical direction

The elastic dynamic response of a high-speed multi-link press is a concern for the designers, and the response value affects the characteristic of mechanism dynamic accuracy. So, the vertical direction response of U on both ends of the link is analyzed. According to the mathematical theory and model parameters above, elastic dynamic response with rotation joint characters or not under different speed are obtained as shown as follows:

As shown in Figs. 10 and 11, with the improvement of the crankshaft speed, elastic dynamics response value of the slider increased. But vertical direction elastic dynamic response without considering rotation joints characters is smaller than the one considering rotation joints characters at the same speed; and with the increase of rotational speed, the growth of dynamic response value with rotation joints characters also becomes bigger.

In the operation process, the designers care more about the elastic dynamic response of the slider near the BDC, and it determines BDC position precision of the press. When the

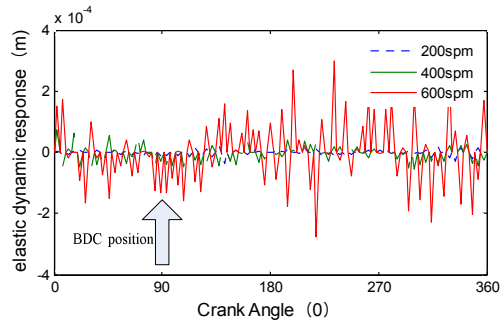

Fig. 10. Elastic dynamic response with rotation joints characteristics.

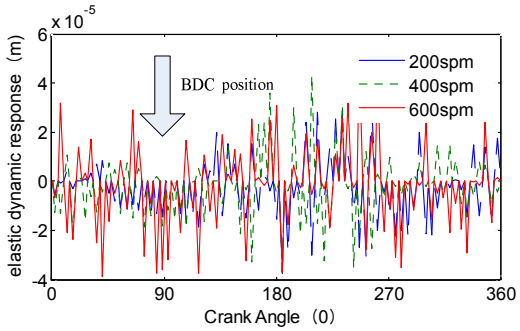

Fig. 11. Elastic dynamic response without rotation joints characteristics.

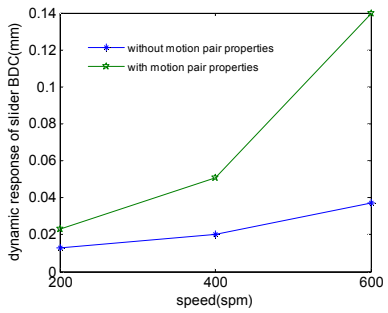

Fig. 12. Dynamic responses of BDC position by two models.

crankshaft angle is 90 degrees, the slider moves to BDC position, and its vertical direction elastic dynamic response value is shown as in the figure. The change of the slider BDC position with the increase of rotation speed is obtained according to Figs. 10 and 11.

As shown in Fig. 12, with the increase of the speed (200-600 spm), the growth of elastic dynamic response value of BDC position is 0.118 mm when considering rotation joint characters. But the elastic dynamic response value without rotation joint characters is smaller, and the growth is 0.027 mm during 200 spm-600 spm.

Therefore, the elastic dynamic analysis method regardless of rotation joint characters cannot explain the elastic dynamic characteristics of high-speed mechanism perfectly. With the speed increase of mechanism, dynamic characteristics of the response value of the low stiffness part are more obvious.

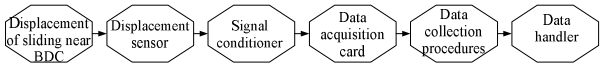

Fig. 13. Testing process of BDC position.

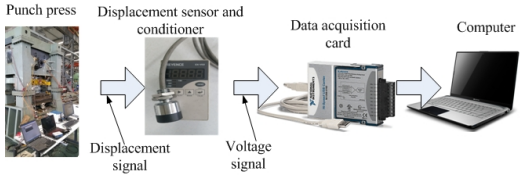

Fig. 14. BDC position test system.

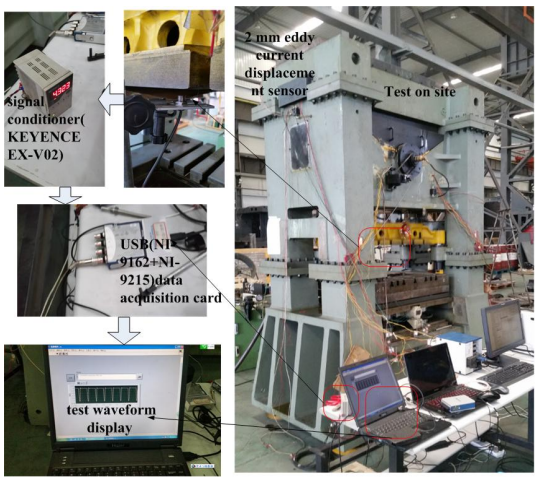

Fig. 15. Test site.

4. Experiment

According to the analysis above, a related test is designed to verify the rationale of the mathematical model. When the slider moves near the BDC, the displacement sensor, data acquisition card and data acquisition program are used to test the BDC position of the mechanism. After the data processing of the collected main slider displacement curve near the BDC, each cycle BDC position is obtained. Then, variable curve of the BDC position can be obtained through data analysis.

Fig. 13 shows the test process of the BDC position. First, displacement of the slider near the BDC is converted into voltage signal by displacement sensor. Second, voltage signal is regulated by displacement signal conditioner. Then, the voltage signal is collected by data acquisition card. In the end, the collected voltage signal is converted to displacement of the slider by data acquisition program, and the real-time display and preservation is done by computer. According to the principle of the above test process of BDC accuracy, the test system is shown in Fig. 14.

The test site is as shown in the figure below:

An eddy current displacement sensor with 2 mm measuring range is used to collect the motion curve of the slider near its BDC position. The sensor is fixed on the working table under the slider as shown in Fig. 15. Lower surface of the slider is

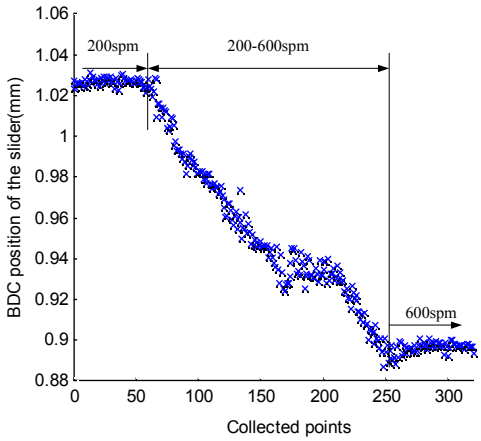

Fig. 16. Collected BDC position of acceleration processes.

used as induction of the electric eddy current displacement sensor. In the process of slider movement (acceleration process from 200-600 spm), the measurement system continuously picks up the signal.

Through the filtering processing of collected data, hundreds of motion curves of the slider near its BDC position can be obtained. The corresponding data processing program is developed to obtain limiting value of each motion curve (i.e., BDC position of the slider) by LabVIEW software. Then the BDC position of the slider during 200-600 spm is collected as shown in Fig. 16.

As shown in Fig. 16, with the increase of speed from 200 to 600 spm, the BDC position reduces 0.13 mm. The speed is accelerated instantaneously, so the influence of temperature on the slider position is negligible. Namely, the change of vertical elastic dynamic response of the press system is around 0.13 mm. The value is similar to the elastic dynamic response with rotation joints characters. However, the elastic dynamic model with perfect kinematic constraints cannot completely reflect the real motion state of the mechanism.

5. Conclusion

(1) An elastic dynamic model of high-speed multi-link press considering structural stiffness of rotation joints is first established in this paper. Comparing elastic dynamic response of improved model with traditional method modeled motion pairs as perfect kinematic constraints, the elastic dynamic response value of the improved model is bigger than the traditional one. With the increase of rotation speed, the growth response value of the traditional elastic method is 0.027 mm. However, the improved model is 0.118 mm.

(2) To validate the rationale of the improved model, a related test was designed. Test results show that the change of BDC position is 0.13 mm with the increase of speed. And it is closer to the response of the improved model, so the improved model considering structural stiffness of rotation joints is more suitable for the research of elastic dynamic characteristics of such high speed mechanism.

Acknowledgment

This work was financially supported by the National Science and Technology Major Project of China (Grant No.2013ZX04002-82), and the national natural science fund project (51275243).

Nomenclature

$\overline{m}$: Equivalent mass matrix
$\overline{k}$: Equivalent stiffness matrix
$\overline{f}$: Generalized force array
$\ddot{u}$: Acceleration array
$\overline{\rho}$: Material density
A : Element cross-sectional area
l : Length of element
$\overline{E}$: Equivalent elastic modulus
F_N : The axial force of bar linkage
$\boldsymbol{B}_i$: Coordinates to coordinate matrix
$\boldsymbol{I}_u(i,k)$: The matrix used to make up the model
C : The damping matrix
spm : Stroke per minute

References

[1] C. K. Toh, Vibration analysis in high speed rough and finish milling hardened steel, *J. Sound Vib.*, 278 (2004) 101-115.
[2] R. Maj, F. Modica and G. Bianchi, Machine tools mechatronic analysis, *Proc. IMechE, Part B: J. Engineering Manufacture*, 220 (2006) 345-353.
[3] S.-S. Yoon et al., Safe arm design with MR-based passive compliant joints and visco-elastic covering for service robot applications, *J. of Mechanical Science and Technology*, 19 (10) (2005) 1835-1845.
[4] H. Chanal, E. Duc and P. Ray, A study of the impact of machine tool structure on machining processes, *Int. J. Mach. Tool Manu.*, 46 (2) (2006) 98-106.
[5] L. Mi et al., Effects of preloads on joints on dynamic stiffness of a whole machine tool structure, *J. of Mechanical Science and Technology*, 26 (2) (2012) 495-508.
[6] I. Zaghbani and V. Songmene, Estimation of machine-tool dynamic parameters during machining operation through operational modal analysis, *Int. J. Mach. Tool Manu*, 49 (12) (2009) 947-957.
[7] Y. N. Lu, L. P. Wang and L. W. Guan, Stiffness analysis and optimization of a hybrid machine tool based on the stiffness matrix, *J. Tsinghua Univ.*, 48 (2) (2008) 180-183.
[8] H. Van Brussel et al., Towards a mechatronic compiler, *IEEE/ASME T. Mech.*, 6 (1) (2001) 90-105.
[9] W. Symens, H. Van Brussel and J. Swevers, Gain-scheduling control of machine tools with varying structural flexibility, *CIRP Ann: Manuf Techn.*, 53 (1) (2004) 321-324.
[10] B. Paijmans et al., Identification of interpolating affine LPV models for mechatronic systems with one varying parameter, *Eur J. Control*, 14 (1) (2008) 16-29.

[11] A. G. Erdman and G. N. Sandor, Kineto-elastodynamics a review of the state of the art and trends, *Mechanism and Machine Theory*, 7 (1) (1972) 19-33.
[12] A. G. Erdman, G. N. Sandor and R. G. Oakberg, A general method for kineto-elastodynamic analysis and synthesis of mechanisms, *J. of Engineering for Industry-Transactions*, 94 (4) (1972) 1193-1205.
[13] P. K. Nath and A. Ghosh, Kineto-elastodynamic analysis of mechanisms by finite element method, *Mechanism and Machine Theory*, 15 (3) (1980) 179-197.
[14] B. V. Viscomi and R. S. Ayre, Nonlinear dynamic response of elastic slider-crank mechanism, *J. of Engineering for Industry-Transactions*, 93 (1) (1971) 251-262.
[15] C.-H. Jou, Dynamic stability of a high-speed slider-crank mechanism with a flexible connecting rod, *M.S. Thesis*, Chung Yuan Christian University, Taiwan (1992).
[16] R.-F. Fung, Dynamic analysis of the flexible connecting rod of a slider-crank mechanism, *ASME J. Vibr. Acoust.*, 118 (4) (1996) 687-689.
[17] R.-F. Fung, Dynamic responses of the flexible connecting rod of a slider-crank mechanism with time-dependent boundary effect, *Comput. Struct.*, 63 (1) (1997) 79-90.
[18] A. A. Shabana and R. Y. Yakoub, Three dimensional absolute nodal coordinate formulation for beam elements: Theory, *J. Mech. Des.*, 123 (4) (2001) 606-613.
[19] R. Y. Yakoub and A. A. Shabana, Three dimensional absolute nodal coordinate formulation for beam elements: Implementation and applications, *J. Mech. Des.*, 123 (4) (2001) 614-621.
[20] M. Berzeri, M. Campanelli and A. A. Shabana, Definition of the elastic forces in the finite-element absolute nodal coordinate formulation and the floating frame of reference formulation, *Multibody Syst. Dyn.*, 5 (1) (2001) 21-54.
[21] M. Berzeri and A. A. Shabana, Development of simple models for the elastic forces in the absolute nodal coordinate formulation, *J. Sound Vib.*, 235 (4) (2000) 539-565.
[22] J. T. Sopanen and A. M. Mikkola, Description of elastic forces in absolute nodal coordinate formulation, *Nonlin Dyn.*, 34 (1) (2003) 53-74.
[23] B. Hussein, D. Negrut and A. A. Shabana, Implicit and explicit integration in the solution of the absolute nodal coordinate differential/algebraic equations, *Nonlin Dyn.,* 54 (4) (2008) 283-296.
[24] O. A. Bauchau and J. Rodriguez, Modeling of joints with clearance in flexible multibody systems, *International J. of Solids and Structures*, 39 (1) (2002) 41-63.
[25] P. Ravn et al., Joint clearances with lubricated long bearings in multibo-dy mechanical systems, *J. Mech. Des.,* 122 (4) (1999) 484-488.
[26] S. Dubowsky, J. F. Deck and H. Costello, The dynamic modeling of fexible spatial machine systems with clearance connections, *J. of Mechanisms, Transmissions and Automation in Design*, 109 (1) (1987) 87-94.
[27] J. F. Deck and S. Dubowsky, On the limitations of predictions of the dynamic response of machines with clearance connections, *Journal of Mechanical Design*, 116 (3) (1994) 833-841.
[28] Z.-L. Ru, H.-B. Zhao and S.-D. Yin, Evaluation of mixed-mode stress intensity factors by extended finite element method, *J. of Central South University*, 20 (5) (2013) 1420-1425.
[29] G. Cheng et al., Finite element method for kinematic analysis of parallel hip joint manipulator, *J. of Mechanisms and Robotics*, 7 (4) (2015) 1502-1512.
[30] G. Wang et al., Dynamics of elastic mechanism considering contact and damping, *J. of Chang'an University (Natural Science Edition)*, 28 (4) (2008) 99-102.
[31] X. Tang et al., Strain rate dependent behaviors of a hot isotropically processed Ti-6Al-4V: Mechanisms and material model, *J. of Mechanical Science and Technology*, 30 (2) (2016) 661-665.
[32] M. Dadashpour et al., Effect of heat treatment and number of passes on the microstructure and mechanical properties of friction stir processed AZ91C magnesium alloy, *J. of Mechanical Science and Technology*, 30 (2) (2016) 667-672.

Fengfeng Hu is a Ph.D. candidate at the School of Mechanical Engineering, Nanjing University of Science and Technology, Nanjing, Jiangsu, P. R. China. His research interests include precision analysis and thermal analysis of mechanisms.

Yu Sun received his Ph.D. from the Nanjing University of Science and Technology, Nanjing, Jiangsu, P. R. China. He is currently a Professor and Doctoral Supervisor in Mechanical Engineering, Nanjing University of Science and Technology. His research interests include manufacturing system, NC forming equipment and Agricultural equipment.

Binbin Peng received his Ph.D. from the Beihang University, Beijing, P. R. China. He is currently an Associate Professor and Master Supervisor in Mechanical Engineering, Nanjing University of Science and Technology, Nanjing, Jiangsu, P. R. China. His research interests include robotics and mechanisms.